

Capturing complex 3D tissue physiology *in vitro*

Linda G. Griffith* and Melody A. Swartz†

Abstract | The emergence of tissue engineering raises new possibilities for the study of complex physiological and pathophysiological processes *in vitro*. Many tools are now available to create 3D tissue models *in vitro*, but the blueprints for what to make have been slower to arrive. We discuss here some of the ‘design principles’ for recreating the interwoven set of biochemical and mechanical cues in the cellular microenvironment, and the methods for implementing them. We emphasize applications that involve epithelial tissues for which 3D models could explain mechanisms of disease or aid in drug development.

Feature

An architectural or compositional component of a scaffold that delineates a distinct, defined region. For example, features in a scaffold with a honeycomb architecture would include: the walls, the hexagonal channels and the overall shape.

Tissue engineering is the process of creating functional 3D tissues using cells combined with scaffolds or devices that facilitate cell growth, organization and differentiation. The field of tissue engineering is at a crossroads. Straight ahead lies the arduous path to successful clinical therapies for replacing human heart, liver, cartilage and other tissues — a road that is arguably longer and more challenging than it seemed about two decades ago when the field sprang to life, as fewer than 10 products have made it to the clinic so far¹. The side road, for now less travelled, leads to engineered tissue and organ mimics that will never be implanted directly into patients, but will instead be used to transform the way we study human tissue physiology and pathophysiology *in vitro*. Indeed, it might decrease the need for organ transplants by enabling the development of therapies that prevent or cure underlying diseases^{2,3}.

Several related factors are driving the field towards the creation of accessible *in vitro* 3D tissue models. One is the need for *in vitro* models that are based on human cells. Although animal models can capture important facets of human responses, they fail to capture others. For example, many pathogens are species specific (for example, hepatitis C), and a leading cause for the failure of new drugs in clinical trials is liver toxicity that was not predicted by animal or *in vitro* models⁴. And, although significant progress has been made in ‘humanizing’ mice by transplanting human cells^{5,6}, such models are currently challenging and expensive to adopt for routine use in an assay format.

Furthermore, fundamental differences in telomerase regulation between rodents and humans⁷ have raised questions regarding the relevance of transgenic and inducible mouse cancer models, and incompatibilities between certain rodent and human cytokines cast uncertainty on human tumour xenograft models. The

development of tissue and quasi-organ *in vitro* models that are based on human cells therefore provides a potential bridge for the gap between animal models and human studies, to help understand the basic mechanisms of human disease. Furthermore, due to the ~US\$1 billion per-compound cost of developing new drugs, 3D tissue models are likely to have an increasingly important role in screening new drugs for efficacy and safety in humans before clinical trials.

Finally, there is an increasing demand for *in vitro* models that capture more of the relevant complexity than traditional 2D cultures can achieve. Individual cells integrate many external cues — including those that arise from various extracellular matrix (ECM) components, mechanical stimulation and soluble signals from adjacent and even distant cells — to generate a basal phenotype and respond to perturbations in their environment. A particular challenge is the coupling of chemical and mechanical signals. Here, we draw from several examples to illustrate how these signals are coupled quantitatively, and describe how advances in synthetic biomaterials, microreactors and quantitative analysis are converging to allow the creation of *in vitro* models that capture some of these complex features of the *in vivo* environment.

The 3D environment

From 2D to 3D. Epithelial cells that exist *in vivo* as multi-layer sheets, such as keratinocytes and corneal epithelial cells, can recapitulate these structures and exhibit differentiated 3D histoarchitecture when cultured on flat substrates in the appropriate culture media^{3,8}, and can mimic the responses of real tissues to drugs and certain toxins well enough to be used in validated toxicology assays^{3,9}.

*Biological Engineering Division, Mechanical Engineering Department and Biotech/Pharma Engineering Center, Massachusetts Institute of Technology, 16-429, 77 Massachusetts Avenue, Cambridge, Massachusetts 02139, USA.
†Institute of Bioengineering, École Polytechnique Fédérale de Lausanne (EPFL), Lausanne, Switzerland
Correspondence to L.G.G.
e-mail: griff@mit.edu
doi:10.1038/nrm1858

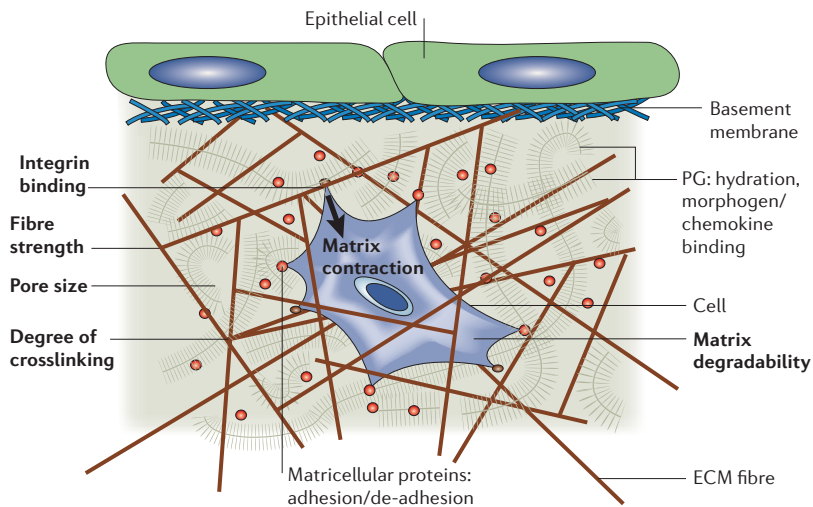


Figure 1 | The importance of the 3D environment for engineering cell function.

The composition, architecture and degree of crosslinking dictate the mechanical properties of the extracellular matrix (ECM) and control how mechanical forces are transmitted to cells. Whereas collagen fibres resist tensional forces and compaction by cells, proteoglycans (PGs) control hydration, which, in turn, determines the resistance to compressive forces, and hinders protein transport by their high, fixed-charge density. Basement membrane, which is secreted basally by epithelial and endothelial cells, further hinders protein transport and increases mechanical stiffness. The matrix composition also controls cell adhesion and migration, and its sensitivity to proteolytic enzymes will determine the ability of the cell to remodel the matrix and migrate through it. Other nonstructural ECM proteins are important for cell function *in vivo*, such as matricellular proteins that support various intermediate states of cell adhesion and de-adhesion to help regulate cell migration, proliferation, apoptosis and differentiation¹²⁸. Because many growth factors, chemokines and other morphogenetic and signalling proteins are secreted in matrix-binding forms, particularly sulphated PGs, the presence of heparin sulphate in the matrix will allow better cellular control of local gradients of such molecules, which can be stored in the matrix and later released proteolytically. Perfusion of the tissue culture will promote nutrient transport and can also impart mechanical stresses on the cells, as well as alter local biochemical gradients (FIG. 2).

Acinar

Pertaining to a sac-like tissue structure in the shape of an acinus, which is a polarized epithelial layer surrounding a small lumen that contains secretions (such as milk) from epithelial cells.

Proteoglycans

Extracellular matrix components that consist of a protein core and glycosaminoglycan side chains. They are huge molecules (> 100 MDa) with a high fixed-charge density and are crucial to maintaining the fluid balance and storing growth factors, cytokines and other morphogens in the matrix.

Most cells, though, require cues from a truly 3D environment to form relevant physiological tissue structures *in vitro*. Culturing cells in 3D versus 2D environments provides another dimension for external mechanical inputs and for cell adhesion, which dramatically affects integrin ligation, cell contraction and associated intracellular signalling^{10,11}. The 3D matrix both affects solute diffusion and binds many effector proteins, such as growth factors and enzymes, thereby establishing tissue-scale solute concentration gradients, as well as local pericellular gradients. Furthermore, the 3D environment might be necessary to model morphogenetic and remodelling events that occur over larger-length scales, such as epithelial acinar formation, and studies of mammary^{12–15} and kidney¹⁶ epithelial-cell behaviour and morphogenesis are good examples of such 3D models (that is, cells seeded within a 3D matrix).

At a basic structural level, tissues comprise a population of cells that interact with each other and with the ECM (FIG. 1). A typical epithelial tissue comprises two parts: a layer of tightly joined, polarized epithelial cells that sits on a thin basement membrane, and an ECM-rich stroma that contains fibroblasts, blood and

lymphatic vessels, and immune cells. The apical surface of the epithelial layer forms a direct barrier against the external environment, or lines the surface of a duct or cyst that stores or carries nutrients or secretions into or out of the body. At the basal surface, epithelia express integrins and other matrix-adhesion molecules that link them to the basement membrane. The stroma both physically supports the epithelial layer and interacts with it through soluble signals and the ECM. The ECM comprises a scaffold of collagens and other structural proteins that is interlaced with proteoglycans, which, together, control the bulk and local mechanical environment, and contribute to the microenvironment through their own signalling moieties and their ability to bind growth factors, cytokines, enzymes and other diffusible molecules (TABLE 1).

Matrix stiffness. Cells exert stresses on their matrix during tissue remodelling, morphogenesis and differentiation, and normal physiological functioning. The matrix stiffness, together with the number of integrin–ligand bonds formed by a cell with its surroundings, dictates the extent to which cells can contract the matrix¹⁷, the ease with which they migrate through it^{18–21} and the degree of intracellular tension that they can generate, which allows them to form stress fibres or organize into acinar structures. The stiffer the matrix, the more difficult it is for cells to contract it, which promotes certain cell functions (such as certain types of endothelial organization²²) and inhibits others.

In breast-epithelial-cell culture, pioneering work by Bissell, Brugge and their co-workers implicated both ECM composition (the engagement of specific adhesion receptors) and ECM stiffness as important regulators of the cellular response^{11–14,23}, providing a foundation for innovative new approaches to shed light on pathophysiological responses^{15,24}. Compared with culturing cells on plastic, on which cells are relatively undifferentiated, cell culture on ECM restores some mammary-specific gene expression. But the greatest degree of morphological and phenotypic similarity to the *in vivo* situation occurs within ECM gels, in which cells proliferate and form acini or ducts^{12,13,25}. Attached collagen gels, which resist forces that are exerted by the cells, foster mammary-cell proliferation. Mammary morphogenesis proceeds only when the collagen gel is released from the substrate and allowed to contract, provided the gel is not too stiff (that is, the collagen concentration is not too high)²⁵. Matrigel, a basement-membrane-like matrix that is rich in laminin, type IV collagen and heparan sulphate proteoglycans, forms more compliant (less stiff) gels than does type I collagen. Therefore, mixing matrigel and collagen I in defined proportions allows relatively constant chemical signals with variable stiffness over a range that is comparable to values that are measured in normal (soft) and malignant (stiff) breast tissues²⁴. For mammary epithelia, increasing the gel stiffness across this range disrupts morphogenesis and enhances proliferation, in part through fostering the phosphorylation of focal adhesion kinase and the formation of focal adhesions, as shown in a recent elegant study by Weaver and co-workers²⁴.

Matrix stiffness also affects the behaviour of fibroblasts, which has further implications in controlling breast-tissue stiffness and therefore mammary-epithelial-cell differentiation. In wound healing and fibrosis, matrix stiffness 'tells' the fibroblasts when and how much to contract¹⁷ (thereby driving their differentiation into myofibroblasts²⁶), as well as the extent to which the wound is contracted or 'healed' (thereby driving reversion to a migratory phenotype²⁷). Normal and irradiated mammary stromal fibroblasts are also responsive to the concentration of collagen in mixtures of collagen and matrigel²⁸. Systematic variation of ligand density and gel stiffness can lead to non-intuitive results, however, and these effects are now being clarified through physical models that incorporate the interplay between cell-generated forces, adhesion-ligand density and matrix stiffness¹⁸. For example, cells that migrate in a soft matrix show an optimal migration speed at lower ligand densities than do cells that migrate in a stiff matrix¹⁸.

Matrix-binding factors. The ECM also binds a wide variety of soluble growth factors and other effector molecules (for example, transforming growth factor- β (TGF β), vascular-endothelial-cell growth factor (VEGF) and hepatocyte growth factor (HGF)^{29,30}), a property that greatly slows their diffusion and therefore serves to fine-tune their local concentrations and gradients. Matrix

binding can create locally higher concentrations of auto-crine growth factors such as heparin-binding epidermal-like growth factor (HB-EGF)³¹, allowing smaller amounts of the factor to signal more effectively³². Likewise, matrix binding might slow the diffusion of paracrine factors to the cells, and together these effects control the balance of autocrine and paracrine signalling dynamics.

Synthetic ECM

Natural ECM gels, such as type I collagen and fibrin, are readily accessible and provide the spectrum of chemical and physical cues that are needed to induce morphogenesis and function from many cells. The diversity of the (often unknown) cues that are present, however, can be a drawback when trying to isolate the effects of specific factors, and natural ECMs can be frustratingly variable in their composition and mechanical properties²⁴. Synthetic gels that are tailored to mimic specific ECM properties are therefore being implemented to provide well controlled and reproducible cellular environments³³ (TABLE 1).

2D gels as a foundation. The first revolution in the direction of synthetic ECM is the widespread adaptation of the 2D system that comprises ligand-modified polyacrylamide gels for the analysis of cell responses to the mechanical properties of the matrix under

Matrigel

Commercially available extract of the basement membrane-like ECM that is secreted by the murine Engelbreth-Holm-Swarm (EHS) tumour and that is rich in laminin, type IV collagen, heparan sulphate proteoglycans and growth factors. It supports the *in vitro* formation of tubes from endothelial cells, as well as the *in vitro* differentiation of many epithelial cell types.

Table 1 | Functional components of the extracellular matrix *in vivo* and their *in vitro* counterparts

<i>In vivo</i> ECM component	Functions	Use of ECM-derived component <i>in vitro</i>	Synthetic mimics*
Collagen: fibrillar (I, II, III, V, XI, XXIV, XXVII)	Structural scaffold Controls stiffness, resists tension Binds adhesion factors (for example, fibronectin) Binds some growth factors (for example, BMP2) Porous: allows amoeboid migration strategies	Reconstituted type I collagen	Electrospun polymer fibres Fibril-forming peptides
Collagen: nonfibrillar (I–XXVII, except fibrillar types)	Broadly serve many ECM and cell-adhesion functions, including: binding other ECM proteins and proteoglycans to aid ECM organization and stability; aiding fibrillar collagen formation; forming networks as barriers for solute transport, including basement membrane (VI); modulating cell migration and proliferation	Matrigel (type IV collagen) Gelatin (denatured fibrillar collagen), adsorbed nonfibrillar collagen components (used mostly for coating 2D surfaces for cell adhesion)	Polymer-bound, short peptide adhesion ligands (for example, Arg–Gly–Asp)
Fibrin	Structural matrix in wound healing Controls stiffness, resists tension Binds adhesion molecules Easily degraded and remodelled	Reconstituted fibrin from blood	Recombinant fibrinogen Fibrinogen derivatives
Elastin	Provides elastic recoil	Reconstituted elastin	Recombinant elastin Elastin-like polypeptides PEO-based gels
Proteoglycans	Resists compression Hinders water transport Hinders macromolecular transport Binds growth factors and chemokines Electrokinetic effects	Hyaluronan Alginate Purified glycosaminoglycans	Alginate derivatives Immobilized heparin Polyelectrolyte gels
Matricellular proteins	Intermediate, weak adhesion (see REF. 127)		Bound peptides and protein subunits

* See REF. 33 for more information. BMP2, Bone morphogenetic protein-2; ECM, extracellular matrix; PEO, polyethylene oxide.

conditions of controlled adhesion-receptor ligation³⁴. By varying the ratio of monomer to crosslinkers, the elastic modulus of polyacrylamide gels cast as thin films on coverslips can be tuned from 100 to 10,000 Pa, a range that is relevant for affecting changes in a wide variety of cells^{24,34–36}. Polyacrylamide gels are highly resistant to protein adsorption and relatively resistant to remodelling by the cells, and can readily be modified with defined and systematically varied concentrations of adhesion molecules. Therefore, they can provide independent control of the natures and number of adhesion sites, as well as the bulk mechanical properties of the adhesion environment. They allow, then, a more direct link of matrix stiffness to phenotype than collagen-matrigel gels, as has been shown for mammary epithelia²⁴.

Designer 3D gels: the frontier is moving mainstream.

Moving to well-defined synthetic 3D systems is far more challenging and requires control not only of cell-adhesion sites and matrix viscoelasticity, but of nano- and microporosity (which regulates cell motility and the transport of soluble molecules), growth-factor binding and matrix degradation. Driven primarily by efforts to address *in vivo* therapeutic applications, significant advances have been made in developing such gels, and they are becoming more accessible as reagents for creating well-controlled 3D environments *in vitro*^{33,37}. For example, self-assembling peptides that gel to form a nanoporous structure with the modulation of salt and pH are now commercially available; these materials offer some control of bulk mechanical properties, and have been used to differentiate stem cells down a hepatic lineage³⁸ and to foster the formation of cartilage from isolated chondrocytes³⁹.

Arguably the most well-defined and adaptable systems are the polyethylene oxide (PEO) macromer-based, peptide-containing gels that were developed by Hubbell and co-workers^{33,40}. Similar to polyacrylamide, PEO strongly resists the nonspecific binding of biological macromolecules and is therefore an ideal base molecular scaffold for creating environments with defined adhesion molecules, growth-factor binding sites and other moieties. Gels can be formed by combining commercially available PEO macromers (activated to react with cysteines) with cysteine-containing peptides under conditions that are mild enough to incorporate cells⁴⁰. In an elegant study to parse the roles of individual chemical and mechanical factors that contribute to 3D cell migration, Raeber *et al.*⁴⁰ used protease-sensitive sequences and peptides containing the Asp–Gly–Arg (RGD) sequence, which enables integrin-mediated adhesion, to create PEO gels with defined concentrations of protease-cleavage sites and adhesion sites, as well as defined mechanical properties and microporosity.

Synthetic ECM is typically designed to stimulate cell adhesion through short peptide sequences that are identified as integrin-binding domains within ECM proteins. The fibronectin-derived RGD-containing peptides are the prototypes, but hundreds of different sequences that are recognized by various integrins and

other adhesion receptors have been identified. Some experimental systems have shown that the cell response might be governed not only by the average ligand concentration, but also by local ligand clustering, which might drive integrin clustering^{41,42}, a phenomenon that has recently been linked to a tumour phenotype in mammary cells²⁴. It is possible that alterations in the properties of the ECM in cancer, such as the upregulation of the multimeric ECM protein **tenascin C**⁴³, might restructure the physical spacing between integrin ligands to alter integrin clustering, a phenomenon that might be investigated further with defined clustering of integrin ligands using gels that allow clustering^{37,41}. Synthetic gels also offer tools for probing growth-factor signalling, as they can covalently incorporate not only growth-factor-binding sites (for example, heparin) that control diffusion, but the growth factors themselves, thereby inhibiting internalization and restricting signalling to the cell surface, or allowing release only by cell-surface proteases^{44,45}. Experimental data on biological responses to matrix-tethered VEGF, epidermal growth factor (EGF), TGF β and others are now emerging^{33,44–46}, allowing the design principles (such as steric factors that might foster or inhibit receptor homodimerization) for the judicious use of these molecules in synthetic ECM to be developed further.

Finally, although technical feasibility might limit the scope of achievable properties in synthetic gels, systems that seem to fall short might still provide adequate cues. For example, mammary-epithelial-cell behaviour is regulated by several β 1 integrins, as well as the non-integrin adhesion receptor dystroglycan¹². Is it necessary to create a gel that contains synthetic ligands for all these receptors and presents them in a physiological stoichiometry and arrangement? Cells secrete their own ECM, which becomes incorporated into the local microenvironment. For example, TGF β 1-mediated deposition of basement membrane by primary Schwann cells in collagen gels is an essential step in creating a microenvironment that fosters their spreading and orientation⁴⁷. So, the synthetic environment might need to provide only an initial set of cues, or a minimal set of dominant cues, to promote a relevant physiological environment.

Molecular gradients in 3D cultures

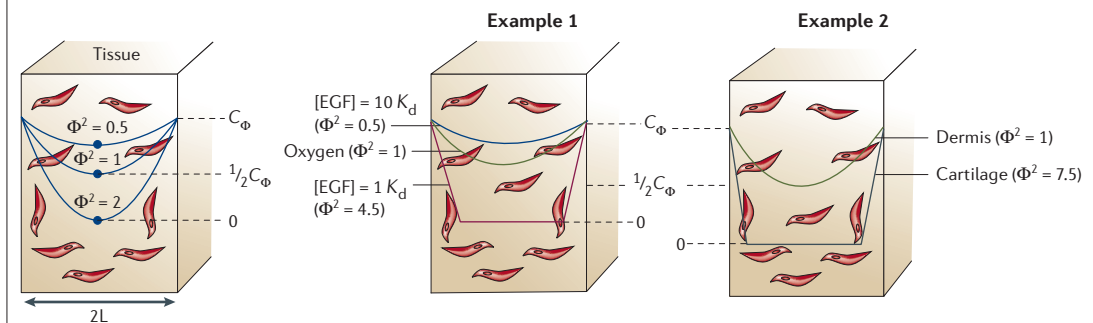
Within a 3D tissue, concentration gradients might exist for any soluble culture-medium component that is consumed or produced by cells — from basic nutrients to effector molecules. These gradients arise from the competition between diffusion and convection with cell consumption or production. The potential impact of these naturally arising concentration profiles on tissue physiology is manifest in two ways: first, because average local concentrations affect local cell behaviours, it can cause cells in the middle of the tissue to behave differently from cells at the surface; and second, it can elicit chemotactic migration or other gradient-dependent cell responses if the transcellular gradient is steep enough for the cell to sense (this condition is typically imposed in chemotaxis studies, but can occur unintentionally).

Convection

Transport by fluid flow (as opposed to diffusion); can refer to the transport of fluid or of solute that is dissolved in the fluid and carried by the flow.

Box 1 | Diffusion and reaction in 3D tissues: estimating the magnitude of concentration profiles

The concentration profile for a substance that diffuses into a slab of tissue and that is being consumed by cells can be estimated by balancing the diffusive transport into the tissue with tissue consumption. In the situation shown, the surface concentration is designated C_0 and the diffusion distance is designated L . The differential balance that relates the local concentration (C), the distance from the tissue surface (x) and the volumetric consumption rate by the tissue (Q) is: $D(d^2C/dx^2) = Q$, where the diffusion coefficient (D) is a constant that has been determined for the particular substance. The solution to this equation for the conditions shown (using a zero-order consumption rate) is $C/C_0 = 1 - \Phi^2[(x/L) - (x/L)^2/2]$ where the equation is cast in dimensionless form to highlight how one parameter, Φ^2 (known as the Thiele modulus), captures the way that changes in the tissue thickness, cell density (that is, the nutrient-consumption rate) and the concentration of the substance at the surface of the tissue influence the concentration profile: $\Phi^2 = (\text{reaction rate})/(\text{diffusion rate}) = L^2Q/(C_0D)$. For $\Phi^2 = 1$, the solution of the equation shows that $C/C_0 = 0.5$ (that is, the concentration of the substance has dropped to 1/2 of its value at the surface of the tissue), and for $\Phi^2 = 2$, the concentration is exactly 0 in the centre. The blue lines in the first box show concentration profiles for various values of Φ^2 , illustrating the rule of thumb that for $\Phi^2 > 1$, significant concentration profiles develop in the tissue. Two examples are shown to illustrate the profiles for some typical culture situations (the relevant data used to calculate Φ^2 for each case are provided in the [Supplementary information S1](#) (box)). In example 1, the concentration profiles are compared for oxygen and epidermal growth factor (EGF) (at an external concentration that is equivalent to $1 K_d$ or $10 K_d$) for fibroblasts at a cell concentration that is comparable to that found in dermis, which illustrates conclusions that are described in the main text. In example 2, oxygen-concentration profiles are compared for cell densities that are representative of dermis and of cartilage, which shows that the higher cell density in cartilage results in oxygen deprivation (experimentally shown in REF. 46).



Basic nutrition. Among basic nutrients, oxygen is usually the most readily depleted due to its relatively low solubility in culture medium, and gradients in glucose and amino acids are almost negligible. Experimental measurements that show oxygen-concentration profiles and their effects on cell viability have been made in several systems^{48,49}. Due to dense cell packing, the oxygen gradients within aggregates of epithelial cells such as hepatocytes, islets and various tumour-cell lines are significant when the aggregate diameter exceeds ~ 0.25 mm in culture medium, whereas the relatively low cell density in stromal tissue (1–10%) results in small oxygen gradients^{48–51}. However, unstirred culture medium is also a significant oxygen diffusion barrier. Even for a 2D-cell monolayer, the oxygen concentration at the cell surface under 2 mm of quiescent culture medium is typically only 10–50% of the concentration at the air–liquid interface (based on the oxygen consumption rate of $4.5 \mu\text{mol}/10^7$ cells/hr for MCF7 mammary cells⁵²), and decreases as the cell concentration increases. (The diffusive flux of oxygen to the monolayer is $D_{\text{oxy}}(C_{\text{surface}} - C_{\text{monolayer}})/h$, where D_{oxy} is the diffusion coefficient of oxygen in culture medium ($2 \times 10^{-5} \text{ cm}^2/\text{s}$), h is the height of the stagnant liquid medium above the cells, and C_{surface} is the oxygen concentration at the air–liquid interface ($\sim 0.15 \mu\text{mol}/\text{cm}^3$). For a confluent monolayer ($\sim 10^5$ cells/ cm^2) under 2 mm of medium, the concentration at the cell monolayer would be $0.025 \mu\text{mol}/\text{cm}^3$, or

$\sim 20\%$ of that at the air–liquid interface.) Local oxygen concentrations regulate cell behaviour in many ways beyond just basic respiration — high oxygen tensions are toxic to many cells, and low oxygen might foster the differentiation of stem cells *in vitro* and *in vivo*^{53–57}. At a molecular level, the cellular-redox state governs the activity of numerous signalling molecules, including tyrosine kinases and phosphatases that are involved in integrin-mediated adhesion through the generation of reactive-oxygen species, a phenomenon that has recently been linked directly to the generation of DNA damage⁵⁸ and to changes in local oxygen concentration⁵⁹.

Efforts to control oxygen delivery to 3D cultures include reducing gradients in the culture medium exterior to the tissue and controlling the dimensions of the tissue. Commercially available cell-culture dish inserts, comprising a flat, semipermeable membrane that lifts the cells near the air–liquid interface and allows nutrients to diffuse up from beneath, help to address this issue. In addition, a wide array of bioreactors that create fluid flow past the tissue surface have been described, including membrane-based reactors (in which cells are cultured outside semipermeable, hollow-fibre membranes), perfusion reactors (in which cells are grown in porous scaffolds and fluid is pumped around them) and stirred-suspension-culture reactors (in which aggregates of cells are kept in suspension)^{51,60–62}. However, most available systems are designed for creating large masses

Box 2 | Technologies for fabricating macroscopic tissue architectures

In the 1990s, the widespread use of computer-aided design and manufacturing across industries as diverse as children's toys and aerospace fostered the development of a broad repertoire of methods to build complex 3D objects in a series of tiny incremental steps that were orchestrated by a computer program — much like inkjet printing creates words on blank paper in 2D, but carried out in sequential layer-by-layer processes (see [Supplementary information S2](#) (box) for a more extensive description of specific methods). Over the past decade, several of these 'rapid prototyping' methods have been adapted to build tissue-engineering scaffolds, as they allow the creation of porous scaffolds with precise internal pore structures and defined macroscopic shapes out of various natural and synthetic biomaterials that are suitable for human implantation, and that can even be used to create large (~10 cm) scaffolds in the specific shape of a particular patient's tissue from a magnetic resonance imaging or computerized tomography scan^{2,125,126}.

Although only relatively simple devices for bone regeneration have yet been successfully deployed in clinical applications, an attractive feature of rapid-prototyping approaches is the potential to vary the composition or pore structure within local regions of a device, thereby providing cues for adhesion and growth of specific cell types in defined patterns^{125–127}. Rapid-prototyping methods are well suited to make large (0.1–10 cm) scaffolds that comprise 0.2–11 mm features (that is, walls and pores and other distinguishing aspects of the structure). This is a suitable resolution for therapeutic applications, in which only rough scaffolds are needed to facilitate tissue ingrowth, but it is perhaps too crude for facilitating the fine-scale cell organization that is desirable for *in vitro* tissue models. Some machines are now commercially available, and can therefore possibly drive this method towards broader applications, although specialized experience is required to adapt the process to specific materials of interest.

of tissue for transplant or extracorporeal treatment and are cumbersome to use for basic science applications, which has motivated the development of microfluidic systems (see below).

Protein regulatory molecules. There are less obvious examples of how important protein-concentration gradients are in 3D tissue behaviour. These include the potential for heterogeneous responses to effector molecules such as EGF, which is often added to culture media at concentrations that are far in excess of its K_d (~1 nM) to ensure receptor saturation. EGF, which stimulates many signalling pathways that govern cell survival, growth, differentiation and motility, is internalized, along with its receptor, after binding to the cell surface. Receptor downregulation and ligand depletion, due to degradation of both ligand and receptor, is a likely outcome for cells that are exposed to 'high' EGF concentrations ($>K_d$), and indeed, such high concentrations will result in near-uniform concentrations throughout a 3-mm-thick gel (BOX 1). However, if the EGF concentration in the medium is adjusted to a concentration that is close to the K_d (1 nM), cells in the interior might be exposed to much lower EGF concentrations.

Engineering analysis. The magnitude of concentration gradients for 3D tissues in the absence of flow can be readily estimated by rules of thumb that derive from a simple mathematical analysis of the competing effects of reaction and diffusion (see equation and examples in BOX 1). The balance is reflected in a single dimensionless parameter, the Thiele modulus

(ϕ^2), that captures the dimensions, reaction rates, diffusion properties and culture-medium concentrations to define the concentration profile in the tissue.

An important barrier to estimating the magnitude of concentration gradients is the lack of available input data — particularly, the rates of consumption and production of regulatory molecules, such as EGF and cytokines. Such data are starting to emerge, driven by phenomenological observations in biology that require quantitative analysis for their understanding⁶³. For example, autocrine loops, once thought to be a hallmark of cancer, are rapidly emerging as primary regulators of cell-signalling networks in homeostasis and disease^{64–67}. Cells use autocrine loops as a kind of sonar system to probe the environment, getting information from what fraction of the signal they send out is recaptured and responding accordingly, thereby possibly helping to define tissue boundaries⁶⁸.

Mathematical models, coupled with controlled experimental measurements, are now starting to unravel how cell density, matrix binding and diffusion affect the ultimate signalling process and are laying the foundation for the rational analysis of more complex 3D systems, in which diffusional transport barriers might allow high levels of autocrine signal to accumulate^{68,69}. The loss of autocrine signalling has also been cited as a factor to explain why high flow rates through 3D tissues, which are intended to improve nutrient transfer, can paradoxically diminish cell survival and function⁷⁰. Clearly, advances in 'cell engineering' (that is, the quantitative analysis of receptor-mediated cell functions) are essential to advance the field of tissue engineering.

Mechanico-chemical signalling

Chemical and mechanical signals are strongly coupled. External mechanical loads are well known to regulate the growth of connective tissues such as bone and muscle — for example, weight-bearing exercise increases tissue mass, whereas space travel reduces it. Likewise, it is well known from studies of such phenomena that external loads are propagated to the cellular level and transmit local molecular forces that stimulate chemical-signalling networks within individual cells. In addition, mechanical stresses are also known to regulate cell behaviour in tissues that are not normally considered mechanically active, often by influencing the spatial distribution of effector molecules in the pericellular environment, thereby effectively coupling mechanical and chemical signalling in every tissue.

Coupling by interstitial flows. *In vivo*, slow interstitial flow is present in all vascularized tissues as an important microcirculatory component between blood and lymphatic capillaries. (As blood flows through capillaries, fluid is forced into the tissue via Starling forces, but not all returns — ~1% of the flow filters through the tissue and drains into lymph, reaching pathological levels during inflammation, and imbalances filtration or lymphatic drainage.) Interstitial fluid

Autocrine loop

Mode of growth-factor signalling in which a cell that expresses a particular growth-factor receptor also synthesizes and releases the corresponding ligand, by which the receptor is activated.

Interstitial flow

Flow through or within the 3D extracellular matrix (as opposed to across a surface or within a vessel).

Starling force

A force that drives fluid movement, including gradients or differences in hydrostatic pressure (which drives fluid flow from higher to lower pressures) and osmotic pressure (which drives fluid flow from less concentrated to more concentrated areas).

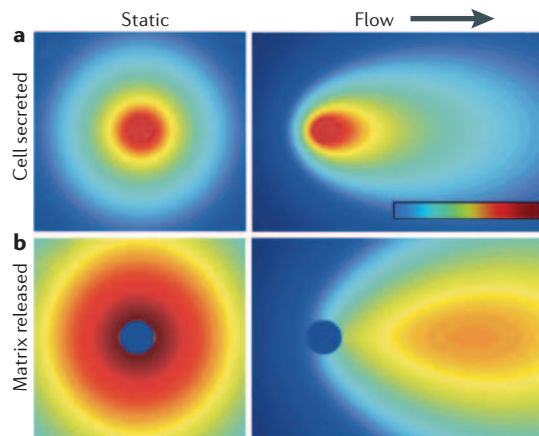


Figure 2 | Coupling between biophysical and biochemical cues. Even subtle mechanical stresses can affect the local extracellular distribution of cell-secreted proteases, morphogens, chemokines and other important proteins, which might give rise to directed cell–cell signalling and anisotropy in engineered tissues. The example shown here is that of a cell-secreted protease releasing matrix-bound morphogen of an average size. **a** | Computational modelling of convection and diffusion of a cell-secreted protease compares the hypothetical steady-state gradients that would result from a flow of $1\ \mu\text{m/s}$ (on the right) versus static conditions (on the left). **b** | Computational estimates of initial relative steady-state matrix-liberated morphogen distribution shows that a transcellular gradient of morphogen can be created under low levels of interstitial flow. So, biophysical forces can induce autocrine chemotactic gradients of matrix-binding factors. The model assumes that free morphogen is generated from the bulk of matrix-bound morphogen in relation to the local protease distribution shown in **(a)**, which then diffuses and convects when liberated. The highest concentration is seen downstream of the cell, because the bulk generation is skewed downstream and compounded by convection of upstream-released morphogen. The colour scale bar shows normalized concentrations from maximum (red) to zero (blue). Modified with permission from REF. 45 © (2005) The National Academy of Sciences; computation by M.E. Fleury.

flow is also stimulated by small mechanical stresses on tissues, and the resulting convection influences the extracellular transport of growth factors, chemokines, proteases and other large molecules. In this way, interstitial flow is an important coupling factor between mechanical stress and signalling in the 3D matrix.

Even the most subtle flows can alter gradients of extracellular molecules that drive cell–cell signalling and morphogenesis. The Peclet number Pe (which equals vL/D ; v , fluid velocity; L , characteristic length (for example, cell diameter); D , diffusion coefficient) describes the ratio of convective to diffusive transport, with convection generally dominating when $Pe > 1$ (although, even when $Pe < 1$, convective forces can still bias the distribution of a molecule^{32,45}). The larger the molecule, the more important fluid convection becomes (relative to diffusion). In the physiological range of convective interstitial flows (~ 0.1 – $1.0\ \mu\text{m/s}$ ^{71,72}), the movement of proteins and

macromolecules is influenced strongly by convection, whereas small solutes (oxygen, glucose) rely mainly on diffusion. Because the actions of chemokines and morphogens depend largely on their local gradients relative to the cell rather than absolute amounts⁷³, interstitial flows are important regulators of tissue behaviour.

For example, Grodzinsky and colleagues^{74,75} have shown that physiological levels of dynamic compression in cartilage strongly influence the deposition patterns of cell-secreted proteoglycans and protease inhibitors. The effects of interstitial flow can be dramatic when numerous molecules are involved, as shown recently in an example of capillary morphogenesis by endothelial cells that are embedded in fibrin gels⁴⁵. Slow interstitial flow (2 – $10\ \mu\text{m/s}$) was observed to act in synergy with matrix-bound VEGF to enhance capillary morphogenesis. Computational modelling showed how this synergy could result from considering the effects of cell-secreted protease, which drove the biased release of VEGF downstream from the cell, creating increasing morphogen gradients in the direction of flow (FIG. 2). As reported recently, VEGF-induced capillary morphogenesis in endothelial cells that are cultured on top of collagen gels can also be influenced by the interplay between the activity of the EGF-receptor autocrine loop and interstitial flow⁷⁶. In this study, both cell survival and capillary formation depended biphasically on interstitial flow, indicating that local gradients in a diffusible EGF-receptor ligand, possibly HB-EGF, contribute to the observed response⁷⁶.

Coupling by externally applied stress. Externally applied mechanical stress not only directly transmits forces to cells (a topic that goes beyond the scope of this review), it changes the relative distances between cells, ECM components and effector molecules. In this way, stretch and compression could directly alter extracellular gradients, cell–cell communication or local concentrations of secreted ligands. This is exemplified in a recent study that showed how changes in autocrine signalling could account for mechanotransduced effects in compressed airway-epithelial cells³¹.

More complex *in vitro* models of human tissues, with two or more cell types that are cultured together in relevant ways, can respond differently to mechanical forces compared with single-cell cultures. First, cells can locally remodel their surroundings (for example, secretion of basement membrane by epithelial cells could stiffen the substrate), resulting in different micromechanical environments that are experienced by different cell types in a shared tissue structure. Second, cells can communicate their respective mechanical environments to each other and respond in a coordinated way to remodel that shared environment⁷⁷. And third, the presence of one cell type can modulate the phenotype and behaviour of the other, leading to unique responses in the co-culture environment. Such complex tissue models are particularly useful for studying pathophysiological responses to environmental stresses, as seen in a recent example of dynamic compressive stress on a 3D human-airway-wall model that induced asthmatic-like remodelling⁷⁸.

Coupling in microvascular flows. Microvascular endothelial cells are also responsive to shear stress *in vitro*, and microvascular homeostasis is partly controlled by fluid flow — for example, an increased need for flow in a tissue leads to the recruitment of quiescent capillaries and, when prolonged, to angiogenesis, whereas decreased flow leads to capillary regression^{79,80}. In a mouse model of skin regeneration, lymphatic capillaries were observed to develop around interstitial fluid channels and in the direction of flow⁸¹. Likewise, interstitial fluid flow can organize single endothelial cells in 3D gels into extensively organized capillary networks^{45,82}. These studies show that functional organization derives naturally from a functional impetus. In light of accumulating evidence that microvessel endothelia help to regulate the function of the underlying tissue^{83–85}, creating functional microvascular networks in 3D *in vitro* models is an important goal.

Coupling might aid tumour-cell escape. Lymphatic transport is the primary route of dissemination for many cancers. Nevertheless, the complex orchestration of matrix proteolysis, chemokine secretion, biophysical forces and other factors that might promote tumour-cell invasion into the lymphatics is still being debated and remains poorly understood^{86–89}. Here, we speculate on how interstitial flows might set up gradients of cell-secreted molecules that direct tumour-cell migration towards lymph or blood capillaries — that is, how coupling between mechanical and chemical signals might aid tumour-cell escape.

Most studies of lymphatic metastasis have used immune-compromised mice with subcutaneously implanted human tumour xenografts, representing a model that does not necessarily grow, invade and metastasize in the same way as a naturally occurring tumour, and omits the important role of immune cells in cancer invasion^{90–92}. Spontaneous tumour models in animals include immune components but inherently lack other specific features of human tumours. *In vitro* physiological 3D models might help to isolate and investigate specific tumour–stromal–lymphatic interactions and extend observations from spontaneous tumour models in animals to the human system.

We speculate that interstitial flow into lymphatics is a crucial component for understanding cell migration towards the lymphatic system. Chemokines that are thought to be important in tumour-cell invasion into the lymphatics, such as CCR7 ligands⁹³, are matrix binding⁹⁴. So, tumour-secreted growth factors and chemokines will both diffuse and convect towards the lymphatic system, but lymphatic-secreted chemokines must diffuse against convection (FIG. 3). Diffusion might still dominate (for example, with an interstitial flow rate of 1 $\mu\text{m/s}$ surrounding the tumour⁷¹, the Peclet number for most growth factors and chemokines, with diffusion coefficients between 20 and 80 $\mu\text{m}^2/\text{s}$, for transport across a cell length, is between 0.25 and 1.0). However, convection can skew the distribution of secreted proteases (in the direction of flow, which is, by definition, directed towards the lymphatic system), and thereby bias the liberation of matrix-bound chemokines and growth

factors to cause autocrine chemotactic gradients — that is, increasing from the downstream to the upstream side of the cell⁴⁵ (FIG. 2). Therefore, because interstitial flow is such a ubiquitous presence that is necessarily directed towards the nearest draining lymphatic vessel, and because it changes the dynamics of cell–cell communication via soluble and matrix-binding factors, we argue that it is an important component in relevant 3D models of tumour–cell–lymphatic interactions.

Interstitial flows might also influence the migration of tumour cells in other ways. Recent data support a model in which mammary carcinoma cells secrete colony-stimulating factor-1 (CSF1), which stimulates macrophages to secrete EGF, causing chemotaxis of carcinoma cells⁹⁵. Interestingly, the tumour cells also secrete at least two matrix-binding autocrine EGFR ligands (HB-EGF and amphiregulin)⁹⁵. It is possible, then, that proteases that are secreted by the macrophages or carcinoma cells could alter the EGFR-ligand environment in ways that will bias migration of carcinoma cells differentially in the presence of interstitial flow compared with static culture, and even possibly create competing gradients of various EGFR ligands *in vivo*.

Frontiers in functional hierarchical tissues

Ideally, based on the analysis provided above of phenomena that occur in tissues, *in vitro* models should comprise a hierarchical arrangement of cells, including microvascular networks within the stroma, and controlled microscale flows not just through the interstitial space, but through blood and lymphatic microvascular networks (and possibly apical ducts). *In vitro* systems that incorporate all these features are still far out on the horizon. However, parallel efforts in scaffold fabrication methods, microreactor technologies and design principles, along with the advances in biomaterials discussed earlier, are contributing to the realization of such complex models.

Tissue engineering scaffolds. A mainstay in tissue engineering is the use of porous scaffolds that provide cells with cues for organization and growth; until recently, such scaffolds have been designed primarily for therapeutic *in vivo* use. Scaffolds might be implanted directly to foster local tissue growth, seeded with cells and implanted immediately, or seeded with cells and cultured *in vitro* to form tissue before implantation^{2,96–100}. Prototypical scaffolds were developed by Yannas and co-workers^{99,101}, who freeze-dried and then crosslinked solutions of collagen and glycosaminoglycans to create biodegradable, sponge-like structures. They controlled fabrication conditions to create a series of scaffolds in which the average pore was systematically varied from about ten microns to several hundred microns. This approach, and many others for creating sponge-like scaffold architectures, have been widely adapted^{2,100}. Surgical fabrics comprising $\sim 10\ \mu\text{m}$ of degradable polyester fibres in felts or weaves were also introduced in the 1980s as therapeutic tissue-engineering scaffolds, and fibre architectures have been likewise widely adapted and extended to a variety of synthetic materials and applications¹⁰⁰.

Fluid shear stress

Mechanical stress on a surface (for example, of a cell or ECM fibre) caused by fluid flow across that surface.

Angiogenesis

The growth of new blood vessels by sprouting from existing vessels in a process that involves endothelial-cell migration and proliferation.

Glycosaminoglycans

Polysaccharide chains of ECM proteoglycans, comprising disaccharide-repeat units with one amino sugar and one negatively charged (carboxylated or sulphated) sugar.

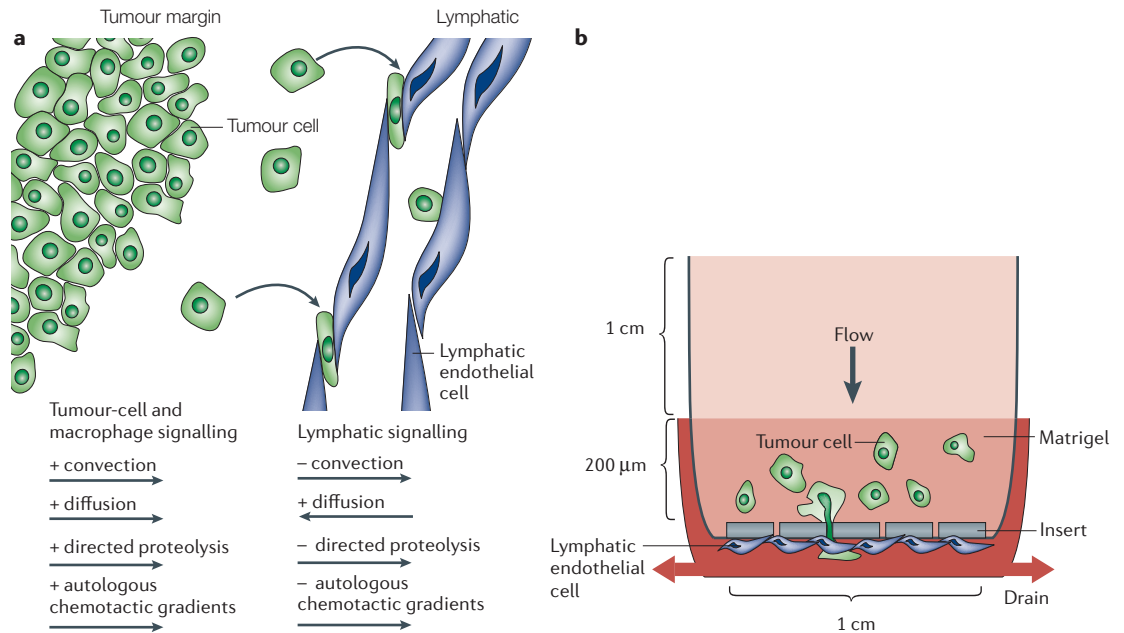


Figure 3 | Biophysical influences on interactions between tumour cells. **a** | The biophysical environment between a tumour margin and its nearest draining lymphatic consists of extracellular matrix (ECM) and slow interstitial-fluid flow (0.1–1.0 $\mu\text{m/s}$) that is always directed from the tumour towards the lymphatic. This flow will affect both the broadcast distances of signalling molecules and their pericellular diffusion gradients. At the tumour-cell margin, chemokines and growth factors that are secreted by tumour cells and macrophages are pushed towards lymphatics by both diffusion and interstitial flow (convection), as indicated by the arrows showing a positive influence for movement towards lymphatics. Furthermore, interstitial flow will bias the distribution of cell-secreted proteases towards lymphatics, promoting directed proteolysis of tumour cells towards lymphatics (positive arrows). At the lymphatics, effector molecules that are secreted by lymphatic cells experience opposing forces on their path towards the tumour — diffusion drives them towards the tumour (positive arrow towards the tumour), but interstitial flow opposes diffusion, thereby blunting lymphatic-secreted signals and hampering lymphatic migration towards the tumour (negative arrows). **b** | The key regulating components of the tumour–lymphatic microenvironment can be simplified in a 3D tissue-culture model. For example, lymphatic endothelial cells (LECs) are cultured in a monolayer on the underside of a small tissue-culture insert (grey), and a gel that contains tumour cells that have formed is placed on top of the insert. A small pressure head of medium maintains interstitial flow (which can be measured and altered by changing the gel thickness). By comparing tumour-cell migration in different conditions (that is, no flow, no LECs, chemokine blocking, invasive versus noninvasive tumour lines, etc.), the interplay between biophysical and biochemical factors that drive lymphatic invasion can be studied.

A general feature of the scaffolds that are described above is an isotropic structure that provides no particular hierarchical tissue organization. These early approaches, and the clinical successes associated with them^{97,98}, stimulated the development of many new methods for fabricating scaffolds with tailored architectures and compositions intended to induce complex tissue architectures. Prominent among these methods are various layer-by-layer fabrication methods (BOX 2), which have also been proposed as an alternative means to create tissues by directly printing cells, thereby forming specific patterns of cells in three dimensions, just as an ink-jet printer creates words on a page by printing dots of ink in two dimensions. Large, low-resolution (0.5–1.0 mm feature size) patterns from certain particularly robust cell types and cell aggregates have been shown¹⁰².

Arguably, there is a fundamental mismatch, however, between the needs of *in vivo* therapeutics and *in vitro* tissue models in the scale of architectural and compositional control that is necessary to create

functional devices. *In vivo*, the ultimate function of the scaffold is almost always to facilitate the natural wound-healing and regeneration processes, with both the local implant site and the body providing a reservoir of cells and effector molecules. So, controlling the structure and composition of a scaffold on dimensions of several tens or hundred microns, and then letting nature take its course, is often adequate. For example, two recent studies showed that endothelial cells that were seeded together with fibroblasts or myoblasts into porous scaffolds formed microvessel-like endothelial networks and, after implantation into nude mice, joined with host microvessels and carried blood^{103,104}. However, it is unclear whether the endothelial structures were functional *in vitro* before they were placed into the proper microenvironment with the right chemical and biophysical cues, including flow. Functionality remains an open question for most microvessel networks that have been observed *in vitro*, and the ability to induce microscale flows in capillaries *in vitro* remains a significant challenge.

Resolution

The smallest dimensions over which the placement or size of a feature can be controlled during the fabrication of a device or scaffold. There are three measures of resolution: positive feature size (the minimum width of a wall that can be created); negative feature size (the minimum possible width of a channel or hole) and feature placement (how reproducible the spacing is between features).

Box 3 | Technologies for creating microscale tissue flows: microfabrication and microfluidics

Microfabrication technologies have grown out of methods that are used to create patterns of conductors, semiconductors and insulators on silicon semiconductor and microelectronic devices, and now encompass a variety of methods that are used to create chemical and topographical patterns on 2D substrates with $\sim 1\ \mu\text{m}$ resolution. A foundation of microfabrication is the ability to place a patterned mask on a silicon wafer and etch away the silicon in the exposed regions to create a topographical pattern (etched trenches and holes), in which features in the pattern are 0.5–500 μm deep. Although silicon devices might be used directly, more commonly, the etched silicon is used as a negative mould to create flexible 3D structures from polydimethylsiloxane (PDMS, or silicone rubber) or other polymers. When the PDMS is removed from the mould, the textured surface can be dipped into a solution that contains molecules that alter cell-substrate adhesion, and is used as a 'stamp' to imprint the pattern onto glass slides or other substrates. PDMS 'stamps' that have been created this way are now widely used to pattern proteins (or other chemicals that alter adhesion) on flat, 2D-culture substrates to control cell adhesion.

However, flexible PDMS structures that are created using a silicon wafer (etched with patterns of trenches and holes) as a mould can be removed from the mould and bonded to glass slides, thereby creating tiny, precise networks of channels in the gaps between the PDMS and the glass — these become 'microfluidic circuits' when fluid is made to flow through them. More generally, microfluidics includes processes and devices that control fluid flow, fluid mixing and chemical reactions in tiny (1–100 μm) channels, conduits and reservoirs that are contained on devices about the size of a microscope slide. Microfluidics allows a complex series of chemical or biochemical reactions to be carried out in a miniaturized format, and often provides enhanced performance due to better control of the molecular and cellular processes at length scales that are comparable to cells, and even molecules.

So, for most *in vitro* applications, it is not clear that the scaffold approaches that are derived from therapeutic tissue engineering currently offer strong advantages over readily accessible and widely used methods, such as the spontaneous organization of cells within the ECM (for example, mammary epithelia embedded in gels with stromal cells^{28,105}) or the creation of heterotypic cell layers with ECM¹⁰⁶. 3D-scaffold-fabrication technologies that are directed at specific *in vitro* needs are beginning to emerge, though, such as the reticulated structures for immune-system engineering that were recently described for T-cell production¹⁰⁷, and the artificial-lymph-node structure for fostering 3D interactions between dendritic cells and T cells¹⁰⁸.

2D microfabrication can create 3D structures. In the pharmaceutical industry, cell-based assays are now routinely used for screening drug safety and efficacy. Indeed, the shortcomings of these assays are an important factor that drives the development of new approaches. High-resolution (0.5 μm) patterns of cell-adhesion proteins or peptides can be created on 2D substrates using microfabrication methods that are borrowed from the microelectronics industry (BOX 3). Cells that are seeded onto patterned substrates adhere only in regions that present the adhesion molecule, and this approach is now widely used to study many adhesion phenomena and cytoskeletal properties of cells in 2D culture¹⁰⁹. Such 2D patterns can be made into 3D tissues by stacking individual layers that are made from thin gels¹¹⁰ or temperature-sensitive adhesion substrates¹¹¹, although handling fragile, thin layers and positioning them correctly relative to each other remain challenging.

3D microfabrication. 3D scaffolds that are formed by etching trenches or holes in thin (0.25–0.5 mm) silicon wafers, or the flexible polymer structures that are created by using such etched silicon as moulds, can be used to organize cells in dimensions that are comparable

to a capillary bed¹¹². The potential of these approaches has been shown by using glass-bonded polydimethylsiloxane (PDMS, or silicone rubber) microchannel structures to create a 3D mimic of an arterial wall, with stacked layers of fibroblasts, smooth-muscle cells and endothelia created within the confines of 0.35-mm-wide microchannels¹¹³, and to create a vascular network that comprises a single, confluent layer of endothelia that lines a predefined network of microchannels¹¹⁴.

Creating microscale flows. The ability to create precisely defined channels and networks of microscale channels in PDMS structures that are bonded to glass has become widely exploited to create interacting microscale flows for carrying out chemical reactions, separating biomolecules and cells, and controlling the behaviour of individual cells^{115,116}. Such microfluidic systems have been used to analyse chemotaxis¹¹⁷, cell adhesion^{118,119} and metabolic interactions between cells that represent different organs, and have been integrated with sensors for oxygen and pH¹²⁰.

A notable advance is the development of microfluidic pumps and valves that can circulate culture medium continuously for weeks through cultures that comprise a few thousand cells, thereby replacing unwieldy peristaltic or syringe pumps¹¹⁹. Microfluidic approaches have been applied primarily to 2D cultures so far, but are starting to be applied to 3D formats⁴. A possible barrier to the widespread use of microfluidic devices for the routine generation of 3D tissues is whether a 'generic' format can be defined that is appropriate for multiple uses and can be commercialized in the way that 96-well plates, sterile filters and other technologies have entered mainstream research. We anticipate that the increasing demands to predict drug safety and efficacy early in the development process will drive this important transition.

Example: 3D microscale-perfused liver. A recent study showed that rat sinusoidal-endothelial cells that are cultured on matrigel form tubes that seem to attract

Capillary bed

A region of tissue that contains a local network of blood microvessels, where the intimate exchange of fluid and molecular components between blood and tissues occurs.

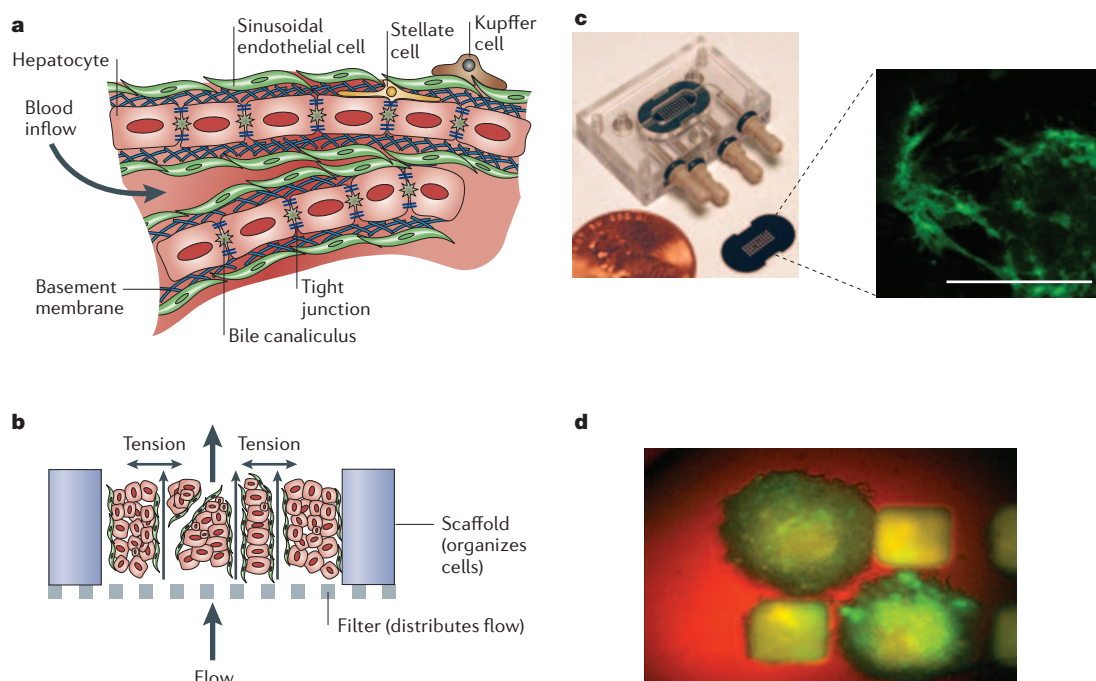


Figure 4 | Microscale 3D model of liver. **a** | The liver capillary bed. Intersecting cords of hepatocytes are separated from blood flowing through sinusoidal capillaries by a wispy basement membrane and highly fenestrated endothelia. Fibroblasts (such as stellate cells) and immune cells (such as Kupffer cells) are present in the sinusoidal lining, and the apical surface appears as tiny bile canaliculi between adjacent hepatocytes¹²⁹. The hepatocyte cords are anchored at the sinusoid inlet by an extracellular-matrix (ECM)-rich stroma that supports the inlet blood supply and bile ducts, and at the outlet by stroma that supports a draining venule (not shown). The architectural requirements are further complicated by a gradient of ECM composition and cell-metabolic activity along the ~0.5 mm length of the sinusoid¹²⁹. **b** | Principles for combining scaffolds with microscale flow to foster the formation and local perfusion of 3D *in vitro* tissue with dimensions that are comparable to that of a liver capillary bed^{4,124}. The scaffold comprises a thin (0.2 mm) silicon or plastic chip with an array of channels that are 0.3 mm wide; each channel serves as the 'functional unit' that is akin to a tissue capillary bed. Cells seeded into the channel are initially held in place by a microporous filter, but soon adhere to the ECM-coated channel walls and form tissue structures. Culture medium is pumped through the tissue at a rate that is governed by tissue oxygen demands and estimates of local shear stress; the filter helps distribute flow uniformly to all channels in the chip. The chip thickness is governed by oxygen needs, whereas the width of the channel is governed by morphogenesis needs. **c** | Liver endothelial cells that are labelled with enhanced green-fluorescent protein form a microvessel network in one channel (out of the 40) of the scaffold when cultured with unlabelled hepatocytes (day 10 of culture; reconstructed multiphoton image; scale = 0.2 mm). **d** | Optical micrograph of a small tumour grown from DU-145 prostate tumour cells that were seeded into an *in vitro* liver bed and cultured for 17 days. The tumour has spilled out of the tissue bed and is growing along the surface of the scaffold (view is enface). Photo in part (c) is courtesy of A. Hwa, P. So, A. Wells, C. Yates, D. Stolz and L. Griffith. Photo in part (d) is courtesy of A. Wells, C. Yates, D. Stolz, S. Watkins and G. Papworth.

Sinusoidal capillary

A discontinuous capillary that consists of endothelial cells with unusually wide gaps between them, and (partially) lacking a basement membrane. Sinusoidal capillaries can be found in liver, spleen and bone marrow.

hepatocytes chemotactically to form tissue-like structures. But, the resulting endothelial networks collapse and disappear within a week of culture initiation¹²¹, which is consistent with other reports that state that the difficulty is maintaining these differentiated endothelial cells alive and functional in culture¹²². We speculate that microscale flow might provide some of the missing signals that are required for liver sinusoidal-endothelial-cell survival. Creating such a model is challenging because of the complex and highly vascularized architecture of the liver (FIG. 4), the relatively high volumetric oxygen-consumption rate of the tissue and the need for long-term culture for applications such as the evaluation of toxicity, gene-delivery efficacy and infection.

As a step in this direction, a microreactor system that fosters the formation of 3D tissue structures from primary rat liver cells that are seeded into a

perfused, microfabricated 3D scaffold has recently been described (FIG. 4), and represents one of the first models that integrates 3D microscale tissue with flow^{4,123,124}. Each tiny channel within the scaffold holds 500–1,000 cells and can be thought of as a functional unit akin to a capillary bed within a tissue bed, and can be scaled to hold 10,000–1,250,000 cells by creating scaffolds with different numbers of channels^{2,4}. Many liver-enriched genes, including drug-metabolizing enzymes that are usually rapidly lost in culture, are maintained in this microreactor system at near-*in vivo* expression and activity levels⁴. This model might therefore be useful in maintaining the local liver microenvironment and fostering the development of perfused microvascular structures that could be used to study phenomena such as the establishment of micrometastases in the liver bed (FIG. 4).

Conclusions and future perspectives

Two foundations that are crucial for the future of the field are now emerging. The first foundation is a set of design principles for building tissues of various tissue types, based on the quantitative analysis of cell and tissue behaviour. We now know a lot about the molecular identity of cell-surface receptors for ECM, other cells and soluble effector molecules. Cell behaviour — which includes survival, motility and differentiation — depends not just on the presence or absence of these cues, but also quantitatively: on their absolute and relative amounts, their spatial arrangements in the cell environment, and the temporal sequence in which they are presented. Engineering analysis allows us to reduce what might seem like an infinite parameter space of cell–environment interactions to ‘cue–signal–response’ rules that allow the fundamental physical and chemical features of

different cues to be captured in predictive mathematical models⁶⁷. At the multicellular or tissue level, engineering analysis allows us to predict how a chemical signal or mechanical force that is provided at a fixed value outside the 3D tissue propagates to individual cells within the tissue and elicits a response.

The second foundation is a toolbox of biomaterials, scaffolds and devices that are used to drive the formation and maintenance of 3D tissue structures *in vitro*, and that can be tailored to specific applications. The development of design principles has arguably lagged behind the development of new materials chemistries and means for fabricating 3D scaffolds — many synthetic approaches were, and still are, based on phenomenological observations. This is changing as the availability of tools to test predictive mathematical and physical models of cell and tissue behaviour increases.

1. Lysaght, M. J. & Hazlehurst, A. L. Tissue engineering: the end of the beginning. *Tissue Eng.* **10**, 309–320 (2004).
2. Griffith, L. G. & Naughton, G. Tissue engineering — current challenges and expanding opportunities. *Science* **295**, 1009–1014 (2002).
3. Suuronen, E. J., Sheardown, H., Newman, K. D., McLaughlin, C. R. & Griffith, M. Building *in vitro* models of organs. *Int. Rev. Cytol.* **244**, 137–173 (2005).
4. Sivaraman, A. *et al.* A microscale *in vitro* physiological model of the liver: predictive screens for drug metabolism and enzyme induction. *Curr. Drug Metab.* **6**, 569–592 (2005).
5. Kuperwasser, C. *et al.* Reconstruction of functionally normal and malignant human breast tissues in mice. *Proc. Natl Acad. Sci. USA* **101**, 4966–4971 (2004).
6. Katoh, M. *et al.* Expression of human phase II enzymes in chimeric mice with humanized liver. *Drug Metab. Dispos.* **33**, 1333–1340 (2005).
7. Rangarajan, A., Hong, S. J., Gifford, A. & Weinberg, R. A. Species- and cell type-specific requirements for cellular transformation. *Cancer Cell* **6**, 171–183 (2004).
8. Watt, F. M. Selective migration of terminally differentiating cells from the basal layer of cultured human epidermis. *J. Cell Biol.* **98**, 16–21 (1984).
9. Louekari, K. Status and prospects of *in vitro* tests in risk assessment. *Altern. Lab. Anim.* **32**, 431–435 (2004).
10. Knight, B. *et al.* Visualizing muscle cell migration *in situ*. *Curr. Biol.* **10**, 576–585 (2000).
11. Roskelley, C. D., Desprez, P. Y. & Bissell, M. J. Extracellular matrix-dependent tissue-specific gene expression in mammary epithelial cells requires both physical and biochemical signal transduction. *Proc. Natl Acad. Sci. USA* **91**, 12378–12382 (1994). **Seminal work that links mammary phenotype to 3D-culture conditions.**
12. Bissell, M. J., Rizki, A. & Mian, I. S. Tissue architecture: the ultimate regulator of breast epithelial function. *Curr. Opin. Cell Biol.* **15**, 753–762 (2003).
13. Debnath, J. & Brugge, J. S. Modelling glandular epithelial cancers in three-dimensional cultures. *Nature Rev. Cancer* **5**, 675–688 (2005).
14. Paszek, M. J. & Weaver, V. M. The tension mounts: mechanics meets morphogenesis and malignancy. *J. Mammary Gland Biol. Neoplasia* **9**, 325–342 (2004).
15. Wozniak, M. A., Desai, R., Solski, P. A., Der, C. J. & Keely, P. J. ROCK-generated contractility regulates breast epithelial cell differentiation in response to the physical properties of a three-dimensional collagen matrix. *J. Cell Biol.* **163**, 583–595 (2003).
16. Zegers, M. M., O'Brien, L. E., Yu, W., Datta, A. & Mostov, K. E. Epithelial polarity and tubulogenesis *in vitro*. *Trends Cell Biol.* **13**, 169–176 (2003).
17. Grinnell, F., Ho, C. H., Lin, Y.-C. & Skuta, G. Differences in the regulation of fibroblast contraction of floating versus stressed collagen matrices. *J. Biol. Chem.* **274**, 918–923 (1999).
18. Zaman, M. H., Kamm, R. D., Matsudaira, P. & Lauffenburger, D. A. Computational model for cell migration in three-dimensional matrices. *Biophys. J.* **89**, 1389–1397 (2005).
19. Lutolf, M. P. *et al.* Synthetic matrix metalloproteinase-sensitive hydrogels for the conduction of tissue regeneration: engineering cell-invasion characteristics. *Proc. Natl Acad. Sci. USA* **100**, 5413–5418 (2003). **Pioneering demonstration of how synthetic extracellular matrices can be tuned to control many facets of cell behaviour in tissue remodelling, using approaches that are accessible to the general cell-biology laboratory.**
20. Lo, C. M., Wang, H. B., Dembo, M. & Wang, Y. L. Cell movement is guided by the rigidity of the substrate. *Biophys. J.* **79**, 144–152 (2000).
21. Peyton, S. R. & Putnam, A. J. Extracellular matrix rigidity governs smooth muscle cell motility in a biphasic fashion. *J. Cell Physiol.* **204**, 198–209 (2005).
22. Sieminski, A. L., Heibel, R. P. & Gooch, K. J. The relative magnitudes of endothelial force generation and matrix stiffness modulate capillary morphogenesis *in vitro*. *Exp. Cell Res.* **297**, 574–584 (2004).
23. Muschler, J. *et al.* A role for dystroglycan in epithelial polarization: loss of function in breast tumor cells. *Cancer Res.* **62**, 7102–7109 (2002).
24. Paszek, M. J. *et al.* Tensional homeostasis and the malignant phenotype. *Cancer Cell* **8**, 241–254 (2005). **Elegant demonstration of a link between matrix mechanics and phenotype in normal and malignant mammary tissue, using a comprehensive range of innovative methods to systematically vary matrix properties *in vitro* to match measured *in vivo* properties, as well as to quantify cell responses.**
25. Wozniak, M. A. & Keely, P. J. Use of three-dimensional collagen gels to study mechanotransduction in T47D breast epithelial cells. *Biol. Proced. Online* **7**, 144–161 (2005).
26. Tomasek, J. J., Gabbiani, G., Hinz, B., Chaponnier, C. & Brown, R. A. Myofibroblasts and mechanoregulation of connective tissue remodelling. *Nature Rev. Mol. Cell Biol.* **3**, 349–363 (2002).
27. Shreiber, D. I., Barocas, V. H. & Tranquillo, R. T. Temporal variations in cell migration and traction during fibroblast-mediated gel compaction. *Biophys. J.* **84**, 4102–4114 (2003).
28. Tsai, K. K., Chuang, E. Y., Little, J. B. & Yuan, Z. M. Cellular mechanisms for low-dose ionizing radiation-induced perturbation of the breast tissue microenvironment. *Cancer Res.* **65**, 6734–6744 (2005).
29. Paralkar, V. M., Vukicevic, S. & Reddi, A. H. Transforming growth factor β type 1 binds to collagen IV of basement membrane matrix: implications for development. *Dev. Biol.* **143**, 303–308 (1991).
30. Ruhrberg, C. *et al.* Spatially restricted patterning cues provided by heparin-binding VEGF-A control blood vessel branching morphogenesis. *Genes Dev.* **16**, 2684–2698 (2002). **This paper showed that heparin-binding VEGF isoforms were necessary for endothelial branching, using transgenic mice that expressed only either matrix-interacting or non-interacting VEGF isoforms.**
31. Tschumperlin, D. *et al.* Mechanotransduction through growth factor shedding into the extracellular space. *Nature* **429**, 83–86 (2004).
32. Swartz, M. A. Signaling in morphogenesis: transport cues in morphogenesis. *Curr. Opin. Biotech.* **14**, 547–550 (2003).
33. Lutolf, M. P. & Hubbell, J. A. Synthetic biomaterials as instructive extracellular microenvironments for morphogenesis in tissue engineering. *Nature Biotechnol.* **23**, 47–55 (2005).
34. Wang, Y. L. & Pelham, R. J. Jr. Preparation of a flexible, porous polyacrylamide substrate for mechanical studies of cultured cells. *Methods Enzymol.* **298**, 489–496 (1998).
35. Reinhart-King, C. A., Dembo, M. & Hammer, D. A. The dynamics and mechanics of endothelial cell spreading. *Biophys. J.* **89**, 676–689 (2005).
36. Semler, E. J., Lancin, P. A., Dasgupta, A. & Moghe, P. V. Engineering hepatocellular morphogenesis and function via ligand-presenting hydrogels with graded mechanical compliance. *Biotechnol. Bioeng.* **89**, 296–307 (2005).
37. Kong, H. J., Polte, T. R., Alsberg, E. & Mooney, D. J. FRET measurements of cell-traction forces and nanoscale clustering of adhesion ligands varied by substrate stiffness. *Proc. Natl Acad. Sci. USA* **102**, 4300–4305 (2005).
38. Semino, C. E., Merok, J. R., Crane, G. G., Panagiotakos, G. & Zhang, S. Functional differentiation of hepatocyte-like spheroid structures from putative liver progenitor cells in three-dimensional peptide scaffolds. *Differentiation* **71**, 262–270 (2003).
39. Kisday, J. *et al.* Self-assembling peptide hydrogel fosters chondrocyte extracellular matrix production and cell division: implications for cartilage tissue repair. *Proc. Natl Acad. Sci. USA* **99**, 9996–10001 (2002).
40. Raebler, G. P., Lutolf, M. P. & Hubbell, J. A. Molecularly engineered PEG hydrogels: a novel model system for proteolytically mediated cell migration. *Biophys. J.* **89**, 1374–1388 (2005).
41. Maheshwari, G., Brown, G., Lauffenburger, D. A., Wells, A. & Griffith, L. G. Cell adhesion and motility depend on nanoscale RGD clustering. *J. Cell Sci.* **113**, 1677–1686 (2000).
42. Coussen, F., Choquet, D., Sheetz, M. P. & Erickson, H. P. Trimmers of the fibronectin cell adhesion domain localize to actin filament bundles and undergo rearward translocation. *J. Cell Sci.* **115**, 2581–2590 (2002).
43. Orend, G. Potential oncogenic action of tenascin-C in tumorigenesis. *Int. J. Biochem. Cell Biol.* **37**, 1066–1083 (2005).

44. Ehrbar, M. *et al.* Cell-demanded liberation of VEGF121 from fibrin implants induces local and controlled blood vessel growth. *Circ. Res.* **94**, 1124–1132 (2004).
- Using protein engineering, this study showed that matrix-binding forms of growth factors led to different signalling patterns, compared with free or unbound growth factors.
45. Helm, C. E., Fleury, M. E., Zisch, A. H., Boschetti, F. & Swartz, M. A. Synergy between interstitial flow and VEGF directs capillary morphogenesis *in vitro* through a gradient amplification mechanism. *Proc. Natl Acad. Sci. USA* **44**, 15779–15784 (2005).
46. Gobin, A. S. & West, J. L. Effects of epidermal growth factor on fibroblast migration through biomimetic hydrogels. *Biotechnol. Prog.* **19**, 1781–1785 (2003).
47. Rosner, B. I., Hang, T. & Tranquillo, R. T. Schwann cell behavior in three-dimensional collagen gels: evidence for differential mechano-transduction and the influence of TGF- β 1 in morphological polarization and differentiation. *Exp. Neurol.* **195**, 81–91 (2005).
48. Kellner, K. *et al.* Determination of oxygen gradients in engineered tissue using a fluorescent sensor. *Biotechnol. Bioeng.* **80**, 73–83 (2002).
49. Glicklis, R., Merchuk, J. C. & Cohen, S. Modeling mass transfer in hepatocyte spheroids via cell viability, spheroid size, and hepatocellular functions. *Biotechnol. Bioeng.* **86**, 672–680 (2004).
50. Gebhardt, R. *et al.* New hepatocyte *in vitro* systems for drug metabolism: metabolic capacity and recommendations for application in basic research and drug development, standard operation procedures. *Drug Metab. Rev.* **35**, 145–213 (2003).
51. Martin, Y. & Vermette, P. Bioreactors for tissue mass culture: design, characterization, and recent advances. *Biomaterials* **26**, 7481–7503 (2005).
52. Guppy, M., Leedman, P., Zu, X. & Russell, V. Contribution by different fuels and metabolic pathways to the total ATP turnover of proliferating MCF-7 breast cancer cells. *Biochem. J.* **364**, 309–315 (2002).
53. Hermitte, F., Brunet de la Grange, P., Belloc, F., Praloran, V. & Ivanovic, Z. Very low O₂ concentration (0.1%) favors G₀ return of dividing CD34⁺ cells. *Stem Cells* **24**, 65–73 (2006).
54. Ezashi, T., Das, P. & Roberts, R. M. Low O₂ tensions and the prevention of differentiation of hES cells. *Proc. Natl Acad. Sci. USA* **102**, 4783–4788 (2005).
55. Wang, D. W., Fermor, B., Gimble, J. M., Awad, H. A. & Guilak, F. Influence of oxygen on the proliferation and metabolism of adipose derived adult stem cells. *J. Cell Physiol.* **204**, 184–191 (2005).
56. Zhao, F. *et al.* Effects of oxygen transport on 3-D human mesenchymal stem cell metabolic activity in perfusion and static cultures: experiments and mathematical model. *Biotechnol. Prog.* **21**, 1269–1280 (2005).
57. Chow, D. C., Wenning, L. A., Miller, W. M. & Papoutsakis, E. T. Modeling pO₂ distributions in the bone marrow hematopoietic compartment. II. Modified Kroghian models. *Biophys. J.* **81**, 685–696 (2001).
58. Radisky, D. C. *et al.* Rac1b and reactive oxygen species mediate MMP-3-induced EMT and genomic instability. *Nature* **436**, 123–127 (2005).
59. Wojciak-Stothard, B., Tsang, L. Y. & Haworth, S. G. Rac and Rho play opposing roles in the regulation of hypoxia/reoxygenation-induced permeability changes in pulmonary artery endothelial cells. *Am. J. Physiol. Lung Cell Mol. Physiol.* **288**, L749–L760 (2005).
60. Morin, J. P., Preterre, D., Keravec, V. & Thuillez, C. Rotating wall vessel as a new *in vitro* shear stress generation system: application to rat coronary endothelial cell cultures. *Cell Biol. Toxicol.* **19**, 227–242 (2003).
61. MacDonald, J. M., Wolfe, S. P., Roy-Chowdhury, I., Kubota, H. & Reid, L. M. Effect of flow configuration and membrane characteristics on membrane fouling in a novel microcoaxial hollow-fiber bioartificial liver. *Ann. NY Acad. Sci.* **944**, 334–343 (2001).
62. Zeilinger, K. *et al.* Time course of primary liver cell reorganization in three-dimensional high-density bioreactors for extracorporeal liver support: an immunohistochemical and ultrastructural study. *Tissue Eng.* **10**, 1113–1124 (2004).
63. Reddy, C. C., Niyogi, S. K., Wells, A., Wiley, H. S. & Lauffenburger, D. A. Engineering EGF for enhanced mitogenic potency. *Nature Biotechnol.* **14**, 1696–1699 (1996).
64. Janowska-Wieczorek, A., Majka, M., Ratajczak, J. & Ratajczak, M. Z. Autocrine/paracrine mechanisms in human hematopoiesis. *Stem Cells* **19**, 99–107 (2001).
65. Prabhu, S. D. Cytokine-induced modulation of cardiac function. *Circ. Res.* **95**, 1140–1153 (2004).
66. Singh, A. B. & Harris, R. C. Autocrine, paracrine and juxtacrine signaling by EGFR ligands. *Cell. Signal.* **17**, 1183–1193 (2005).
67. Janes, K. A. *et al.* A systems model of signaling identifies a molecular basis set for cytokine-induced apoptosis. *Science* **310**, 1646–1653 (2005).
68. DeWitt, A. *et al.* Affinity regulates spatial range of EGF receptor autocrine ligand binding. *Dev. Biol.* **250**, 305–316 (2002).
- Determined quantitative properties that govern tissue distribution of secreted growth factors.
69. Wiley, H. S., Shvartsman, S. Y. & Lauffenburger, D. A. Computational modeling of the EGF-receptor system: a paradigm for systems biology. *Trends Cell Biol.* **13**, 43–50 (2003).
70. Cartmell, S. H., Porter, B. D., Garcia, A. J. & Guldberg, R. E. Effects of medium perfusion rate on cell-seeded three-dimensional bone constructs *in vitro*. *Tissue Eng.* **9**, 1197–1203 (2003).
71. Chary, S. R. & Jain, R. K. Direct measurement of interstitial convection and diffusion of albumin in normal and neoplastic tissues by fluorescence photobleaching. *Proc. Natl Acad. Sci. USA* **86**, 5385–5389 (1989).
72. Dafni, H., Israely, T., Bhujwalla, Z. M., Benjamin, L. E. & Neeman, M. Overexpression of vascular endothelial growth factor 165 drives peritumor interstitial convection and induces lymphatic drain: magnetic resonance imaging, confocal microscopy, and histological tracking of triple-labeled albumin. *Cancer Res.* **62**, 6731–6739 (2002).
73. Gurdon, J. B. & Bourillot, P. Y. Morphogen gradient interpretation. *Nature* **413**, 797–803 (2001).
74. Quinn, T. M., Grodzinsky, A. J., Buschmann, M. D., Kim, Y. J. & Hunziker, E. B. Mechanical compression alters proteoglycan deposition and matrix deformation around individual cells in cartilage explants. *J. Cell Sci.* **111**, 575–583 (1998).
75. Garcia, A. M., Lark, M. W., Trippel, S. B. & Grodzinsky, A. J. Transport of tissue inhibitor of metalloproteinases-1 through cartilage: Contributions of fluid flow and electrical migration. *J. Orthop. Res.* **16**, 734–742 (1998).
76. Semino, C. E., Kamm, R. D. & Lauffenburger, D. A. Autocrine EGF receptor activation mediates endothelial cell migration and vascular morphogenesis induced by VEGF under interstitial flow. *Exp. Cell Res.* **312**, 289–298 (2006).
77. Swartz, M. A., Tschumperlin, D. J., Kamm, R. D. & Drazin, J. M. Mechanical stress is communicated between cell types to elicit matrix remodeling. *Proc. Natl Acad. Sci. USA* **98**, 6180–6185 (2001).
78. Choe, M. M., Sporn, P. H. S. & Swartz, M. A. An *in vitro* airway wall model of remodeling. *Am. J. Physiol. Lung Cell Physiol.* **285**, L427–L433 (2003).
79. Popel, A. S. & Johnson, P. C. Microcirculation and microheology. *Ann. Rev. Fluid Mech.* **37**, 43–69 (2005).
80. Schmid-Schonbein, G. W. Biomechanics of microcirculatory blood perfusion. *Annu. Rev. Biomed. Eng.* **1**, 73–102 (1999).
81. Boardman, K. C. & Swartz, M. A. Interstitial flow as a guide for lymphangiogenesis. *Circ. Res.* **92**, 801–808 (2003).
82. Ng, C. P., Helm, C. L. & Swartz, M. A. Interstitial flow differentially stimulates blood and lymphatic endothelial cell morphogenesis *in vitro*. *Microvasc. Res.* **68**, 258–264 (2004).
83. LeCouter, J. *et al.* Angiogenesis-independent endothelial protection of liver: role of VEGFR-1. *Science* **299**, 890–893 (2003).
84. Shin, V., Zebboudj, A. F. & Bostrom, K. Endothelial cells modulate osteogenesis in calcifying vascular cells. *J. Vasc. Res.* **41**, 193–201 (2004).
85. Matsumoto, K., Yoshitomi, H., Roussant, J. & Zaret, K. Liver organogenesis promoted by endothelial cells prior to vascular function. *Science* **294**, 559–563 (2001).
86. Cao, Y. Emerging mechanisms of tumour lymphangiogenesis and lymphatic metastasis. *Nature Rev. Cancer* **5**, 735–743 (2005).
87. Swartz, M. A. & Skobe, M. Lymphatic function, lymphangiogenesis, and cancer metastasis. *Microsc. Res. Tech.* **55**, 92–99 (2001).
88. Saharinen, P., Tammela, T., Karkkainen, M. J. & Alitalo, K. Lymphatic vasculature: development, molecular regulation and role in tumor metastasis and inflammation. *Trends Immunol.* **25**, 387–395 (2004).
89. Van Trappen, P. O. & Pepper, M. S. Lymphatic dissemination of tumour cells and the formation of micrometastases. *Lancet Oncol.* **3**, 44–52 (2002).
90. Balkwill, F. Cancer and the chemokine network. *Nature Rev. Cancer* **4**, 540–550 (2004).
91. Mougel, L. *et al.* Three-dimensional culture and multidrug resistance: effects on immune reactivity of MCF-7 cells by monocytes. *Anticancer Res.* **24**, 935–941 (2004).
92. Elgert, K. D., Alleva, D. G. & Mullins, D. W. Tumor-induced immune dysfunction: The macrophage connection. *J. Leukoc. Biol.* **64**, 275–290 (1998).
93. Wiley, H. E., Gonzalez, E. B., Maki, W., Wu, M. T. & Hwang, S. T. Expression of CC chemokine receptor-7 and regional lymph node metastasis of B16 murine melanoma. *J. Natl Cancer Inst.* **93**, 1638–1643 (2001).
94. Patel, D. D. *et al.* Chemokines have diverse abilities to form solid phase gradients. *Clin. Immunol.* **99**, 43–52 (2001).
95. Goswami, S. *et al.* Macrophages promote the invasion of breast carcinoma cells via a colony-stimulating factor-1/epidermal growth factor paracrine loop. *Cancer Res.* **65**, 5278–5283 (2005).
- Compelling evidence of a cell-generated chemotactic gradient that operates in 3D on a heterotypic cell type.
96. Muschler, G. F., Nakamoto, C. & Griffith, L. G. Engineering principles of clinical cell-based tissue engineering. *J. Bone Joint Surg. Am.* **86-A**, 1541–1558 (2004).
97. Stern, R., McPherson, M. & Longaker, M. T. Histologic study of artificial skin used in the treatment of full-thickness thermal injury. *J. Burn Care Rehabil.* **11**, 7–13 (1990).
98. Mansbridge, J., Liu, K., Patch, R., Symons, K. & Pinney, E. Three-dimensional fibroblast culture implant for the treatment of diabetic foot ulcers: metabolic activity and therapeutic range. *Tissue Eng.* **4**, 403–414 (1998).
99. Yannas, I. V. Synthesis of tissues and organs. *ChemBioChem* **5**, 26–39 (2004).
100. Stock, U. A. & Vacanti, J. P. Tissue engineering: current state and prospects. *Annu. Rev. Med.* **52**, 443–451 (2001).
101. Yannas, I. V., Lee, E., Orgill, D. P., Skrabut, E. M. & Murphy, G. F. Synthesis and characterization of a model extracellular matrix that induces partial regeneration of adult mammalian skin. *Proc. Natl Acad. Sci. USA* **86**, 933–937 (1989).
- Pioneering demonstration of design principles that are applied to the development of synthetic scaffolds for tissue regeneration.
102. Jakab, K., Neagu, A., Mironov, V., Markwald, R. R. & Forgacs, G. Engineering biological structures of prescribed shape using self-assembling multicellular systems. *Proc. Natl Acad. Sci. USA* **101**, 2864–2869 (2004).
103. Tremblay, P. L., Hudon, V., Berthod, F., Germain, L. & Auger, F. A. Inoculation of tissue-engineered capillaries with the host's vasculature in a reconstructed skin transplanted on mice. *Am. J. Transplant.* **5**, 1002–1010 (2005).
104. Levenberg, S. *et al.* Engineering vascularized skeletal muscle tissue. *Nature Biotechnol.* **23**, 879–884 (2005).
105. Tlsty, T. D. & Hein, P. W. Know thy neighbor: stromal cells can contribute oncogenic signals. *Curr. Opin. Genet. Dev.* **11**, 54–59 (2001).
106. Jasmund, I. & Bader, A. Bioreactor developments for tissue engineering applications by the example of the bioartificial liver. *Adv. Biochem. Eng. Biotechnol.* **74**, 99–109 (2002).
107. Poznansky, M. C. *et al.* Efficient generation of human T cells from a tissue-engineered thymic organoid. *Nature Biotechnol.* **18**, 729–734 (2000).
108. Stachowiak, A. N., Bershteyn, A. & Irvine, D. J. Bioactive hydrogels with an ordered cellular structure combine interconnected macroporosity and robust mechanical properties. *Adv. Mater.* **17**, 399–403 (2005).
- Demonstration of an innovative approach in creating synthetic scaffolds for the recreation of complex tissue behaviours *in vitro*.

109. Whitesides, G. M., Ostuni, E., Takayama, S., Jiang, X. & Ingber, D. E. Soft lithography in biology and biochemistry. *Annu. Rev. Biomed. Eng.* **3**, 335–373 (2001).
110. Klebe, R. J. Cytoscribing: a method for micropositioning cells and the construction of two- and three-dimensional synthetic tissues. *Exp. Cell Res.* **179**, 362–373 (1988).
111. Tsuda, Y. *et al.* The use of patterned dual thermoresponsive surfaces for the collective recovery as co-cultured cell sheets. *Biomaterials* **26**, 1885–1893 (2005).
112. Andersson, H. & van den Berg, A. Microfabrication and microfluidics for tissue engineering: state of the art and future opportunities. *Lab Chip* **4**, 98–103 (2004).
113. Tan, W. & Desai, T. A. Microscale multilayer cocultures for biomimetic blood vessels. *J. Biomed. Mater. Res. A* **72**, 146–160 (2005).
114. Shin, M. *et al.* Endothelialized networks with a vascular geometry in microfabricated poly(dimethyl siloxane). *Biomed. Microdevices* **6**, 269–278 (2004).
115. Weibel, D. B., Garstecki, P. & Whitesides, G. M. Combining microscience and neurobiology. *Curr. Opin. Neurobiol.* **15**, 560–567 (2005).
116. Hansen, C. & Quake, S. R. Microfluidics in structural biology: smaller, faster em leader better. *Curr. Opin. Struct. Biol.* **13**, 538–544 (2003).
117. Lin, F. *et al.* Neutrophil migration in opposing chemoattractant gradients using microfluidic chemotaxis devices. *Ann. Biomed. Eng.* **33**, 475–482 (2005).
118. Lu, H. *et al.* Microfluidic shear devices for quantitative analysis of cell adhesion. *Anal. Chem.* **76**, 5257–5264 (2004).
119. Song, J. W. *et al.* Computer-controlled microcirculatory support system for endothelial cell culture and shearing. *Anal. Chem.* **77**, 3993–3999 (2005).
120. Sin, A. *et al.* The design and fabrication of three-chamber microscale cell culture analog devices with integrated dissolved oxygen sensors. *Biotechnol. Prog.* **20**, 338–345 (2004).
Shows the principles of multi-compartment tissue models 'on a chip', incorporating many principles of microfabrication and microfluidics.
121. Yaakov, N., Schwartz, R. E., Hu, W.-S., Verfaillie, C. & Odde, D. J. Endothelium-mediated hepatocyte recruitment in the establishment of liver-like tissue *in vitro*. *Tissue Eng.* (in the press).
122. DeLeve, L. D., Wang, X., Hu, L., McCuskey, M. K. & McCuskey, R. S. Rat liver sinusoidal endothelial cell phenotype is maintained by paracrine and autocrine regulation. *Am. J. Physiol. Gastrointest. Liver Physiol.* **287**, G757–G763 (2004).
123. Powers, M. J. *et al.* Functional behavior of primary rat liver cells in a three-dimensional perfused microarray bioreactor. *Tissue Eng.* **8**, 499–513 (2002).
124. Powers, M. J. *et al.* A microfabricated array bioreactor for perfused 3D liver culture. *Biotechnol. Bioeng.* **78**, 257–269 (2002).
125. Lin, C. Y., Kikuchi, N. & Hollister, S. J. A novel method for biomaterial scaffold internal architecture design to match bone elastic properties with desired porosity. *J. Biomech.* **37**, 623–636 (2004).
126. Yeong, W. Y., Chua, C. K., Leong, K. F. & Chandrasekaran, M. Rapid prototyping in tissue engineering: challenges and potential. *Trends Biotechnol.* **22**, 643–652 (2004).
127. Sherwood, J. K. *et al.* A three-dimensional osteochondral composite scaffold for articular cartilage repair. *Biomaterials* **23**, 4739–4751 (2002).
128. Bornstein, P. & Sage, E. H. Matricellular proteins: extracellular modulators of cell function. *Curr. Opin. Cell Biol.* **14**, 608–616 (2002).
129. Sigal, S. H., Brill, S., Fiorino, A. S. & Reid, L. M. The liver as a stem cell and lineage system. *Am. J. Physiol.* **263**, G139–G148 (1992).

Acknowledgements

We thank A. Hwa, A. Wells, D. Stolz, S. Watkins, C. Yates, G. Papworth and P.T. So for the use of unpublished photos. We thank D. Lauffenburger, F. Gertler and V. Weaver for critical review of the manuscript.

Competing interests statement

The authors declare no competing financial interests.

DATABASES

The following terms in this article are linked online to:
UniProtKB: <http://ca.expasy.org/sprot>
CSF1 | HB-EGF | HGF | tenascin C | TGFβ | VEGF

FURTHER INFORMATION

Linda Griffith's homepage: <http://biomicro.mit.edu/research/griffith.html>

SUPPLEMENTARY INFORMATION

See online article: S1 (box) | S2 (box)
Access to this links box is available online.